ELSEVIER

Journal of Nuclear Materials 276 (2000) 33–40

journal of nuclear materials

www.elsevier.nl/locate/jnucmat

Dislocation loop structure, energy and mobility of self-interstitial atom clusters in bcc iron

B.D. Wirth[a,*], G.R. Odette[a,c], D. Maroudas[b], G.E. Lucas[a,b]

[a] *Department of Mechanical Engineering, University of California, Santa Barbara, CA 93106, USA*
[b] *Department of Chemical Engineering, University of California, Santa Barbara, CA 93106, USA*
[c] *Department of Materials Engineering, University of California, Santa Barbara, CA 93106, USA*

Abstract

Molecular-statics and molecular-dynamics (MD) simulations based on the embedded-atom method (EAM) were used to model the energy and mobility of self-interstitial atom (SIA) clusters in bcc α-iron. Isolated SIAs and SIA clusters, directly produced in displacement cascades have significant impact on the microstructural evolution under neutron and high-energy charged particle beam irradiations. The SIA clusters are composed of ⟨1 1 1⟩ split dumbbells and crowdions bound by energies in excess of 1 eV. The clusters can be described as perfect prismatic dislocation loops with Burgers vector $\mathbf{b} = (a/2)\langle 1\,1\,1\rangle$. As the loops grow, SIAs fill successive jogged edge rows, with minimum free energy cusps found at the 'magic' numbers corresponding to un-jogged filled hexagonal shells. The total energy of the clusters is in excellent agreement with continuum elasticity dislocation theory predictions. However, the core region is extended compared to an isolated edge dislocation. The extended regions are preferentially located at the hexagonal corners of the loop, forming intrinsic kinks. As a result of the intrinsic kinks, the SIA clusters are highly mobile and undergo one-dimensional motion on their glide prism. The high cluster mobility is related to the easy motion of the edge segments which propagate the kinks along the loop periphery resulting in increments of prismatic glide. The corresponding activation energy for SIA cluster diffusion is less than 0.1 eV. Linking atomistic point defect cluster calculations dislocation theory provides a powerful tool in understanding radiation damage.

1. Introduction

The structure and mobility of self-interstitial atom (SIA) clusters has profound significance on microstructural evolution in irradiated materials. Numerous authors have shown that high-energy displacement cascades initially develop and cool over picosecond time scales, resulting in a shell of SIAs and SIA clusters surrounding a vacancy-rich core. A significant fraction of SIAs reside in larger than 4-atom clusters [1–6]. A wide range of irradiation effects, that occur over time scales up to 10^9 s, are mediated by the transport and ultimate fate of the primary cascade defects.

Thus, developing a good understanding of the production, character, energy, and mobility of the primary defects is a very important objective. For example, the structure, energetics and dynamics of SIA clusters are important in addressing the following questions: the net number and configuration of residual defects during the initial correlated recombination and subsequent long-term aging of cascades [7–9]; the absence of small, observable dislocation loops in ferritic materials in low-temperature, low-dose irradiations [10]; the source and mechanism of point defect cluster hardening, including effects on post yield strain hardening [11–13]; cluster-decorated dislocation structures [14]; and vacancy and interstitial sink strength and bias [11,15,16]. This paper reports an extensive simulation study of the structure and energetics of the SIA clusters in pure bcc α-iron, as well as a semi-quantitative characterization of their mobility.

* Corresponding author. Present address: Chemistry and Materials Science Division, Lawrence Livermore National Laboratory, P.O. Box 808, L-353, Livermore, CA 94551, USA. Tel.: +1-925 424 9822; fax: +1-925 422 7040.
E-mail address: wirth4@llnl.gov (B.D. Wirth)

0022-3115/00/$ - see front matter
PII: S0022-3115(99)00166-X

High-mobility SIA clusters have been observed in a number of molecular-dynamics (MD) studies and have been studied by several groups [6,17–24]. For example, Osetsky and co-workers also find high mobility of $\langle 1\,1\,1\rangle$ SIA clusters in α-Fe [22–24]. They attribute the mobility to be largely the consequence of the collective effect of the individual motion of crowdions. In contrast, this work links the structure of SIA clusters to perfect (unfaulted) prismatic (hexagonal) dislocation loops, whose energies are well described by continuum elasticity[1] dislocation theory. Such loops are clearly glissile; and their very high mobility can be related to the existence and easy, and likely correlated, motion of kinked edge segments. While the end results are similar, the unification of dislocation and point defect views has significant conceptual and practical advantages, such as in the treatment of long-range drift forces, cluster trapping by solute atoms, and the mechanisms of sink interactions.

2. Calculational methods

Clusters containing up to 91 SIAs were studied using a Finnis–Sinclair type many-body interatomic potential [25], as modified by Calder and Bacon [4]. The ground-state structure and formation energy of the clusters was evaluated with a variant of the simulated annealing method [26]. This structural relaxation scheme involved isothermal-isobaric metropolis Monte Carlo (MC) simulations at each annealing stage in conjunction with conjugate gradient quenching. Isothermal-isobaric MD simulations were used to evaluate the mobility of SIA clusters. Both the MC and MD simulations were carried out using a modified version of the MOLDY code [27]. Periodic boundary conditions were applied to supercells containing from 2000 to 54 000 atoms. Insensitivity of the results to the supercell size was used to ensure that the effects of interactions of a cluster with its periodic images were negligible.

3. Results and discussion

3.1. SIA cluster structure and energetics

For the interatomic potential used in this study, the lowest-energy configuration of an isolated SIA is a $\langle 1\,1\,0\rangle$ split dumbbell [17–19]. Two metastable configurations have energies very near to that of the ground state energy. The $\langle 1\,1\,1\rangle$ split dumbbell has a formation energy only 0.11 eV higher, while the so-called $\langle 1\,1\,1\rangle$ crowdion SIA configuration is only 0.15 eV higher. Crowdions and split dumbbells are defined as arrays of atoms in the close packed $\langle 1\,1\,1\rangle$ direction, where m atoms share $m-1$ lattice sites. If m is even, the center of mass of the array is located at a lattice site and the configuration is a $\langle 1\,1\,1\rangle$ split dumbbell; if m is odd, the center of mass is located symmetrically between two lattice sites and the configuration is a $\langle 1\,1\,1\rangle$ crowdion. The alternate $\langle 1\,1\,1\rangle$ configurations are separated by a translation of $a/4\,\langle 1\,1\,1\rangle$ and the crowdion is the saddle-point configuration for migration of the $\langle 1\,1\,1\rangle$ split dumbbell [17–19].

Clusters of $N \geqslant 2$ SIA with $\langle 1\,1\,0\rangle$ orientations have very high energies associated with extensive strain field overlap. However, in the $\langle 1\,1\,1\rangle$ cluster configuration, compressive and tensile dilation centers align in a much lower energy state. Minimum-energy configurations are found when the clusters are composed of mixtures of $\langle 1\,1\,1\rangle$ split dumbbells and crowdions. The centers of mass of the SIAs lie in an extended (>2) set of $\{1\,1\,0\}$ planes. The structure and energies of small SIA clusters have been reported elsewhere [17–19,21]. In the remainder of this paper, the focus is on the characteristics of larger clusters ($7 \leqslant N \leqslant 91$). The simulations focused on a particularly stable subset of SIA clusters, consisting of n successive filled hexagonal shells surrounding a central SIA with a total number N_n of 7, 19, 37, 61, 91, ..., $N_{n-1} + 6(n-1)$ SIAs, $n \geqslant 2$. These so-called 'magic number' clusters produce cusps in the formation energy curve associated with the absence of a jog on one of the hexagonal segments that occurs at other cluster sizes, N.

Fig. 1(a) and (b) show $[1\,1\,\bar{1}]$ and $[0\,0\,1]$ projections, respectively, of clusters containing 19 and 91 SIAs with formation energies of 43.7 and 116.8 eV, respectively. The circles are the centers of mass of the extended arrays of atoms in the $\langle 1\,1\,1\rangle$ direction; filled circles correspond to crowdions, while the open circles are $\langle 1\,1\,1\rangle$ split dumbbells. Notably, the $[1\,1\,\bar{1}]$ projection shown in Fig. 1(a) describes a prismatic dislocation loop, bounded by $(a/2)\,\langle 1\,1\,1\rangle$ edge dislocation segments. A Burgers circuit analysis yields the expected $(a/2)\,\langle 1\,1\,1\rangle$ Burgers vector. However, the clusters are more extended than a perfect *planar* prismatic dislocation loop, located on only two additional $(2\,2\,0)$ planes. Both the 19- and 91-member SIA clusters occupy six $(2\,2\,0)$ planes, as illustrated in Fig. 1(c). The extended cluster locations correspond to the presence of intrinsic kinks. Extended kinks are observed around the periphery of the loop, but appear to be preferentially located at the hexagonal corners. Kinks on diagonal corners frequently have opposite signs.

The description of the kinked prismatic dislocation loop character of SIA clusters can unify the atomistic, point-defect descriptions of these features with the much more general framework of dislocation theory. For example, the fact that the ground state of such a loop is intrinsically kinked is not conceptually surprising

[1] In our analysis dislocation core energies are incorporated into continuum elasticity dislocation theory.

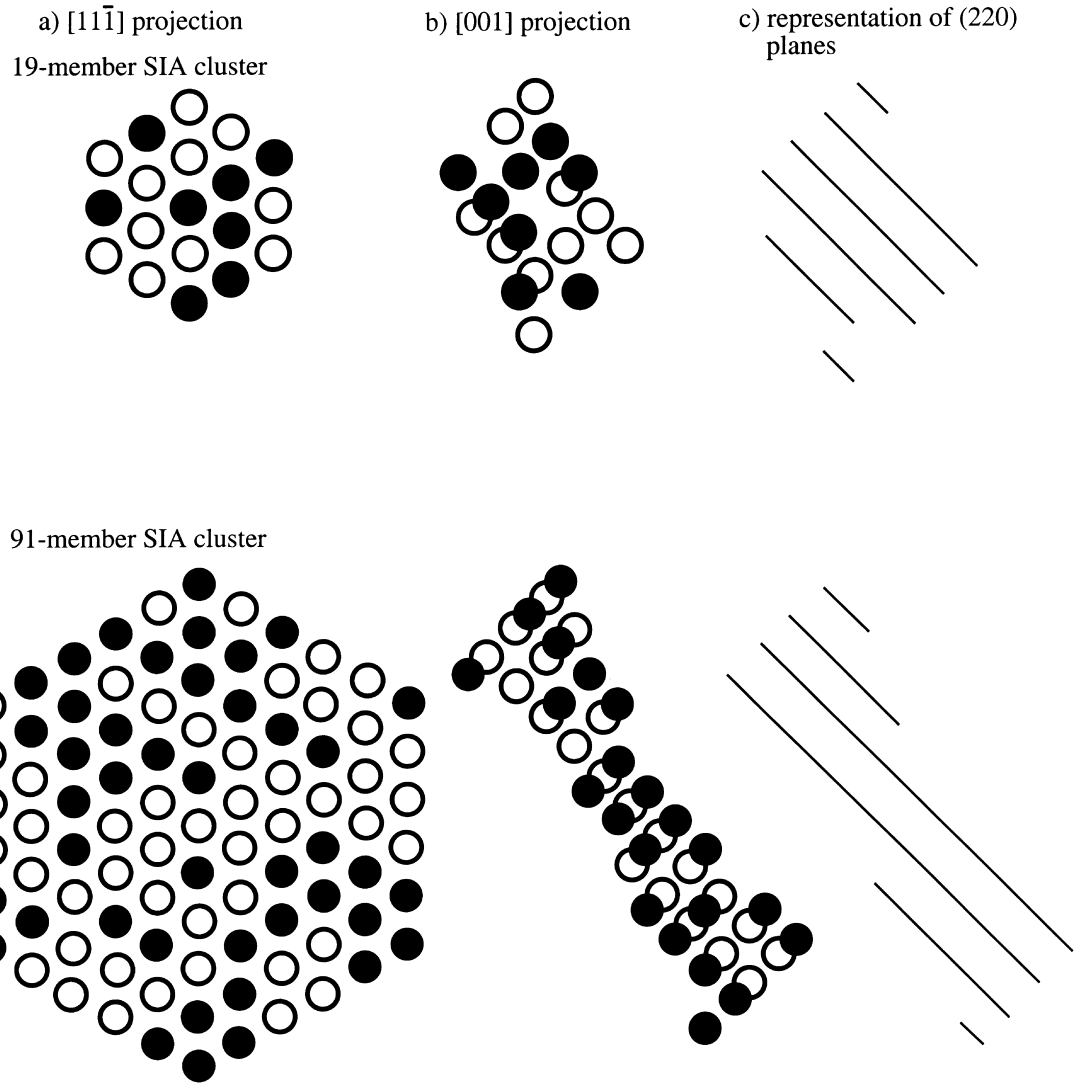

Fig. 1. 19- and 91-member SIA clusters in (a) [1 1 $\bar{1}$] and (b) [0 0 1] projection. Filled and open circles represent the centers of mass of ⟨1 1 1⟩ crowdions and split dumbbells, respectively. (c) Additional (2 2 0) lattice planes occupied by the clusters.

considering the strong self-interaction energies, much akin to the symmetrically kinked segments in dislocation dipoles [28]. More generally, according to this view, both the formation energy and mobility of the clusters can be described in terms of the corresponding characteristics of dislocations, such as energy per unit length, mobility and jog and kink energy.

The practical significance of the loop-like character of small-to-intermediate sized SIA clusters to details of the corresponding energies and mobilities must address the following question. Does continuum elasticity dislocation theory provide a good quantitative description of the key features of SIA clusters found from atomistic-level MD and MC simulations? The rest of this paper will focus on this question.

The first and simplest test of the dislocation loop view is to compare the total cluster energy from the atomistic simulations to the corresponding prediction of continuum elasticity theory. Hirth and Lothe derive an expression for the self-energy, E_{hex}, of a prismatic hexagonal dislocation loop as [28]

$$E_{\text{hex}} = \frac{6\mu b^2 L}{4\pi(1-\nu)}\left[\ln\left(\frac{L}{\rho}\right) + C\right]. \quad (1)$$

In Eq. (1), μ is the shear modulus of the bulk material, ν the Poisson ratio, b the magnitude of the dislocation Burgers vector, L the length of the hexagonal loop edge, ρ a dislocation core cutoff radius, and C represents a constant dislocation core energy plus a

small contribution for interactions between the dislocation segments. The dependence of E_{hex} on L as predicted by Eq. (1) is shown as the dashed line in Fig. 2, where C was taken as a fitting parameter. The average relaxed values of the hexagonal segment length, $\langle L \rangle$, were determined from the atomistic simulations. Using nominal values of $\mu = 83$ GPa and $\nu = 0.29$, $b = 0.248$ nm for bcc iron and a recommended value of $\rho = 0.72$nm [28], a value of C equivalent to a core energy of about 4 eV/nm provides a very good fit to the formation energies, E^f, of the 'magic' self-interstitial clusters. This value of C is consistent with earlier computer simulation studies based on pair potentials, yielding a range of core energies from 4 to 6 eV/nm [29]. Note that, a 50% increase in the fitted core energy results in only a 10–20% increase in the continuum predictions of E_{hex} according to Eq. (1). The non-magic number SIA clusters have an average excess energy of about 1.1 eV relative to a fit of the magic number E^f vs. $N^{1/2}$.[2] This is consistent with estimates of an edge dislocation jog energy of about 1.2 eV [28].

In summary, both the structure of SIA clusters and the close agreement between their total energy, found from the atomistic simulations, and the corresponding predictions of continuum elasticity dislocation theory with a dislocation core energy fitted to the atomistic simulation results, lend considerable support to the viewpoint that SIA clusters act as hexagonal loops, even down to very small sizes.

3.2. SIA cluster migration

Detailed MD simulations of the migration of the single SIA and small ($N \leqslant 4$) SIA clusters over a range of temperatures have been reported previously [17,19,20]. For the interatomic potential used in this work, single SIAs undergo a multiple-step migration process involving rotations between the $\langle 1\,1\,0 \rangle$ and $\langle 1\,1\,1 \rangle$-oriented split dumbbell configurations followed by $\langle 1\,1\,1 \rangle$ translation through the crowdion saddle point. The process is complicated in that the sequence of jumps is not random, but favors the direction of the previous motion. The overall migration behavior is governed by such correlation effects and the detailed balance of rotations in and out of the $\langle 1\,1\,1 \rangle$ orientation. Note that, as is also discussed in more detail elsewhere [19], as the temperature increases the $\langle 1\,1\,1 \rangle$ orientation is increasingly populated. Above about 400 K this configuration becomes the lowest-energy state [19,21].

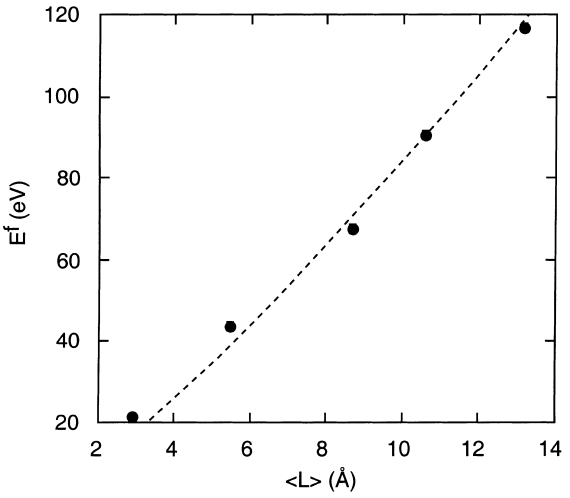

Fig. 2. Formation energy of the magic clusters of sizes $N = 7$, 19, 37, 61, and 91 as a function of the corresponding hexagonal loop average edge length $\langle L \rangle$. The dashed line is a least-squares fit according to continuum dislocation theory, Eq. (1), where the dislocation core energy is the only fitting parameter.

Small SIA clusters undergo similar collective one-dimensional migration along $\langle 1\,1\,1 \rangle$ with a low activation energy barrier that can be described as the 'local' disassociation and re-association of the cluster which moves in an 'amoebae-like' fashion. Di-interstitial clusters are able to rotate into other $\langle 1\,1\,1 \rangle$ orientations [17]. The probability of rotation versus migration falls to low values for cluster sizes above $N = 2$ on the MD simulation time scale (on the order of 100 ps).

MD simulations performed at a temperature of 560 K also reveal a common migration mechanism for the larger ($19 \leqslant N \leqslant 91$) SIA clusters/loops. The most salient feature of the migration process is that, just as for the single SIAs and smaller SIA clusters, in all cases cluster migration occurs as a highly anisotropic, one-dimensional quasi-diffusive type motion with a very low activation energy. For example, individual sequences for 19- and 91-member clusters showed net displacements of 4.9 nm after 25 ps and about 6 nm in 135 ps, respectively [18,19]. As in the case of single SIAs, sequences of several correlated jumps appear to be biased in the same direction.

Limited MD simulations of 19- and 37-member SIA clusters over the temperature range from $100 \leqslant T \leqslant 900$ K for 200 ps were carried out to assess semi-quantitatively a *nominal* loop diffusion coefficient, D_L, and migration activation energy, E_L. Fig. 3 shows the

[2] Based on the simplest geometric arguments, the total energy of magic number clusters would scale as $N^{1/2}$ or the total loop circumference. Indeed, this scaling provides an excellent fit to the magic number simulation data, though similar fitting results also can be obtained for other scaling (e.g., $N^{2/3}$). However, the simple geometric picture is modified by factors such as self-interaction energies and significant volume relaxation that occurs in SIA clustering. In the fits to continuum dislocation theory, these effects are accounted for by using average relaxed hexagonal segment lengths.

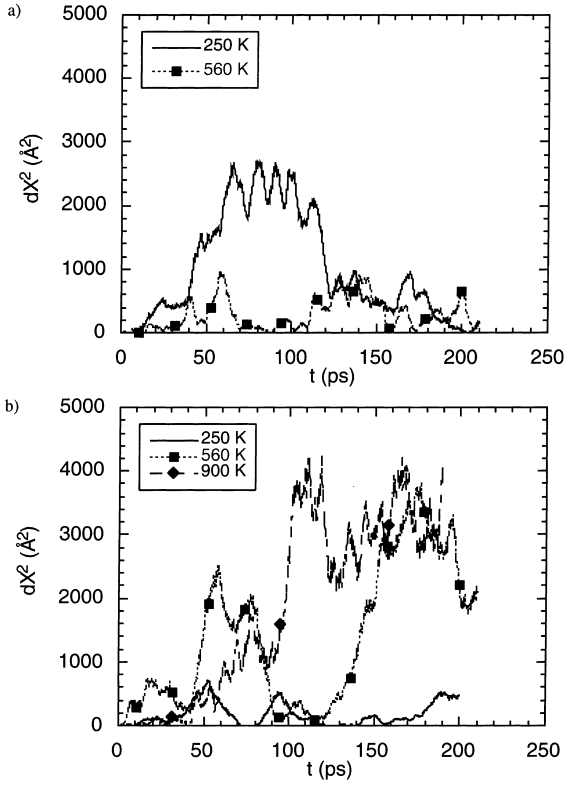

Fig. 3. Evolution of squared displacement of the SIA cluster center of mass as computed through MD simulations at several temperatures for (a) 19-member and (b) 37-member SIA clusters.

corresponding squared displacements of the center of mass of the SIA clusters of size 19 and 37, ΔX^2, plotted at fixed time intervals of 0.1 ps, for various simulation temperatures. The mean squared displacements, $\langle \Delta X^2 \rangle_i$, over 25 ps time intervals were used to estimate D_L[3] as the average of 8 $\Delta X_i^2/25$ ps segment (i) values. Since the migration process involves non-conventional, correlated jumps, and since the statistics is associated with only a few (8) relatively short (≈600 jumps) trajectories, D_L is approximate at best.[4] However, this procedure should provide reasonable order-of-magnitude estimates of the cluster mobility parameters.

Fig. 4 shows the Arrhenius plots of $D_L(T)$ for the 19- and 37-member clusters. The migration activation energy fit for the 19-member cluster is 0.023 eV with a pre-factor of 1.7×10^{-7} m^2/s. The migration activation

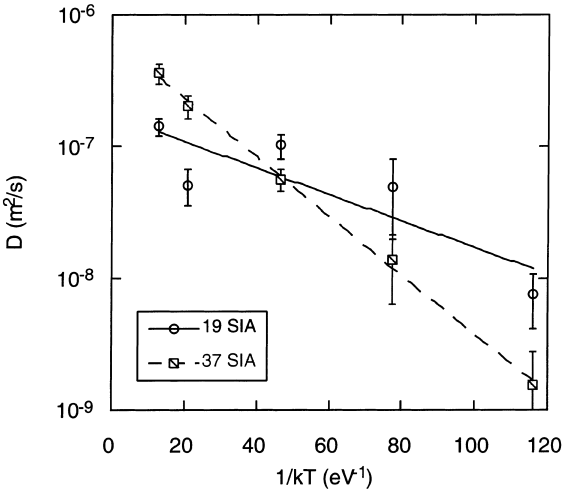

Fig. 4. Temperature dependence of the diffusivity of the 19- and 37-member SIA clusters, calculated by averaging over 25 ps sub-trajectories.

energy fit for the 37-member cluster is 0.052 eV with a pre-factor of 6.5×10^{-7} m^2/s. These results indicate that the smaller cluster is more mobile at low temperatures, as expected. However, the relative mobility reverses for temperatures above about 250 K. This may be a real effect or simply an artifact due to the large uncertainties in evaluating D_L. However, in all cases, including the 91-member cluster, the mobility can be characterized as extremely high above 100 K, even on MD (on the order of 100 ps) time scales.

The fact that SIA clusters relax into intrinsically kinked prismatic loop configurations also explains their high mobility. It is well established that edge motion occurs approximately athermally or with a very low activation energy [28]. Thus, motion of loop edge segments on glide prisms will induce movement of kinks around its periphery. In small to medium sized loops, with strong interactions between the line segments and hexagonal corners, this process is likely to be correlated, in the sense that the kinks move under the influence of one another, rather than independently.

Low-temperature MD simulations were performed in an attempt to retard cluster motion and characterize the migration mechanism in detail. At a temperature of 75 K, the 37-member cluster does not move over 150 ps. This is consistent with a activation energy of migration of about 0.05 eV; specifically, the corresponding diffusional time scale, τ, based on the estimated value of D_L is $\tau = b^2/(2D_L) \approx 150$ ps.

Detailed monitoring of the evolution of the center of mass of the SIAs forming the loop shows clearly kink propagation about the periphery. Fig. 5 shows four snapshots from a MD simulation at 100 K over intervals of 0.3 ps during which the loop propagates a distance of

[3] $D_L = \langle \Delta X^2 \rangle_i / 2t$ for one-dimensional migration.

[4] Monte Carlo diffusion simulation reveals that averaging over multiple (≈100) trajectories is required to obtain a linear relation of $\langle X^2 \rangle$ vs time. Significant variance occurs from this mean in any particular trajectory [19].

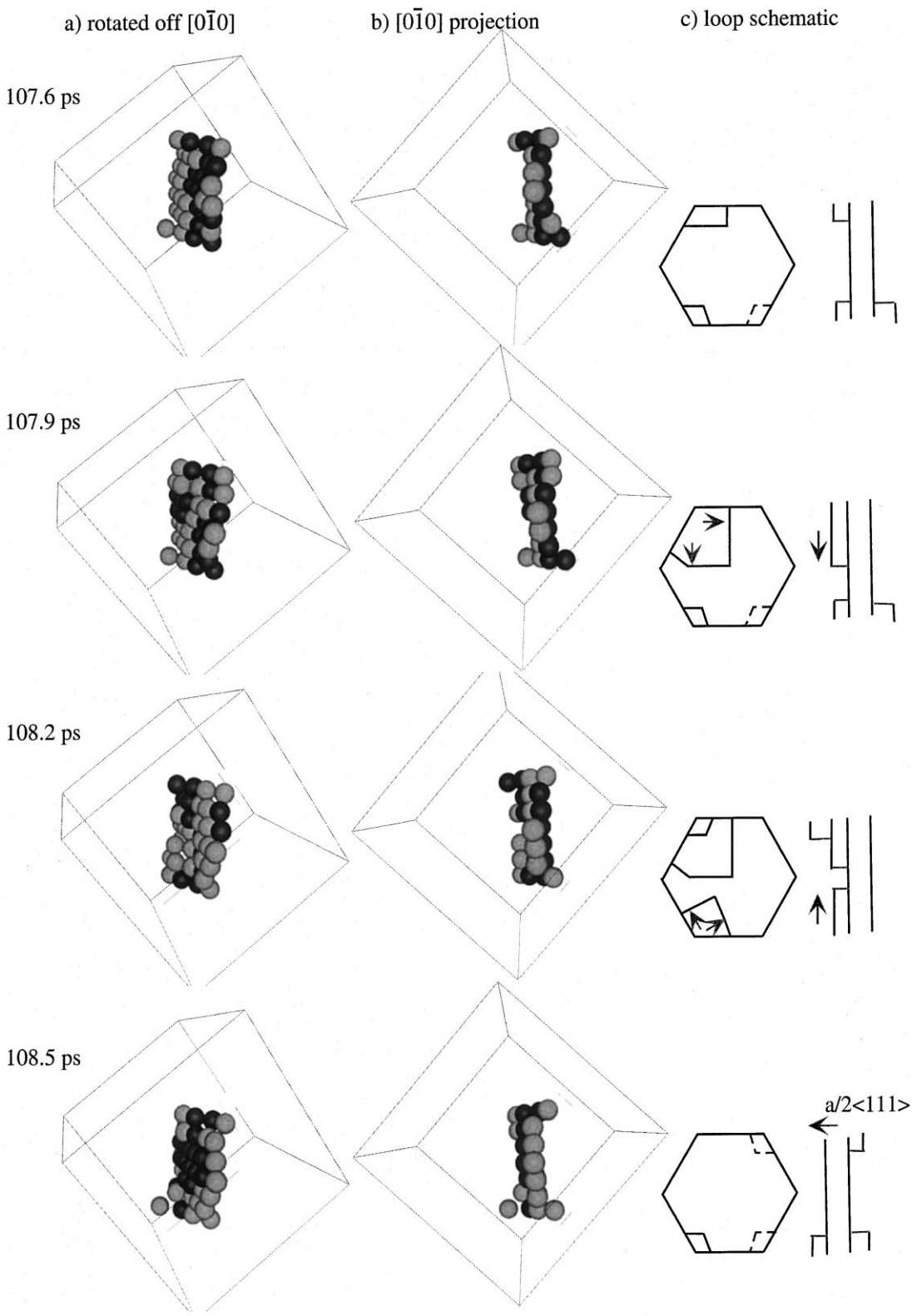
a) rotated off [0$\bar{1}$0]
b) [0$\bar{1}$0] projection
c) loop schematic
107.6 ps
107.9 ps
108.2 ps
108.5 ps
a/2<111>

Fig. 5. MD simulation snapshots of a 37-member SIA cluster at 100 K at times of 107.6, 107.9, 108.2, and 108.5 ps viewed from: (a) a projection rotated slightly off $[0\ \bar{1}\ 0]$; (b) an $[0\ \bar{1}\ 0]$ projection; and (c) by schematically illustrating the motion of the hexagon and additional loop half-planes. Light and dark gray filled spheres denote the centers of mass of $\langle 1\,1\,1\rangle$ crowdions and split dumbbells, respectively.

$(a/2)\ \langle 1\,1\,1\rangle$ (from right to left). Fig. 5(a) is a projection, slightly rotated off $[0\ \bar{1}\ 0]$. Fig. 5(b) shows an edge-on, $[0\ \bar{1}\ 0]$ projection to demonstrate the atomic movement of the additional cluster half-planes. Fig. 5(c) shows a schematic representation of loop migration, projecting both along the Burgers vector (illustrating the cluster hexagon) and edge-on (illustrating the extra half-planes). The loop initially has two corner kinks in the reverse direction (right to left) shown by solid lines and one in the forward direction shown by the dashed line. Over the next 0.3 ps, the kink in the upper left corner begins to propagate around the periphery. By 0.6 ps an additional reverse kink has formed in the upper left corner, while the lower left (reverse) kink begins to propagate around the loop and the forward kink disappears. Over the next 0.3 ps, the original, reverse directed kinks coalesce propagating the loop by one Burgers vector along the glide direction (in the reverse sense, from right to left). The second, upper-left (reverse) corner kink disappears and three kinks reform in corners, two in the forward and one in the reverse direction.

The effect of cluster size on mobility has not been quantified yet. However, it is clear that mobility will decrease with increasing N for at least two reasons: (a) the probability of intrinsic kinks is expected to decrease with increasing loop size; and (b) the time, τ_k, needed for the motion of kinks to produce a net cluster displacement increases with increasing loop size and the mobility scales as τ_k^{-1}. Considering process (b), two limiting cases can be envisioned: (i) random kink diffusion with $\tau_k^{-1} \propto \langle L\rangle^{-2}$ approximately scaling with N^{-1}; and (ii) highly correlated kink drift motion with $\tau_k^{-1} \propto \langle L\rangle^{-1}$ approximately scaling with $N^{-1/2}$. While the cluster mobility intrinsically decreases with increasing size, other extrinsic factors, including those affected by the loop size, like trapping by solutes, are expected to have a much more profound effect on the overall loop migration rates.

4. Conclusions and implications

As noted previously, existing viewpoints on small SIA clusters range from an emphasis on their point defect (crowdion) character [22–24], to focus on their prismatic loop-type structure and properties. The differences in viewpoints have more than semantic consequence. In particular, the continuum dislocation elasticity viewpoint can be linked to a wide range of highly developed theories and models of dislocation physics. For example, trapping of gliding loops by individual solute atoms or solute atmospheres can be readily treated within the dislocation framework [28,30]. So can loop drift in response to various sources of internal stress, as well as certain aspects of loop interactions with sinks. Furthermore, while the detailed results are uncertain due to factors such as the interatomic potential and computational limitations, the dislocation viewpoint links point defect cluster physics to the much more robust and experimentally buttressed understanding of dislocation mechanics and dynamics. In this regard, it is noted that Osetsky and co-workers find that $\langle 1\,1\,1\rangle$ vacancy loops in α-iron are also very mobile [23]. This is consistent with a prismatic loop description, but would seem hard to rationalize solely from the perspective of a cluster of crowdions.

There are, of course, a number of unresolved questions, including: determination of quantitative diffusion coefficient pre-exponential factors and activation energies, including possible effects of correlated processes; the effect of the approximate isotropic interatomic potential; how loops annihilate at sinks; and, how loop mobility quantitatively varies with size. Answers to these and other important questions will require additional research.

Acknowledgements

This work was supported by the US Nuclear Regulatory Commission under contract number NRC-04-94-049.

References

[1] A. Seeger, in: Proceedings of the Second UN International Conference on Peaceful Uses of Atomic Energy, vol. 6, Geneva, United Nations, New York, 1958, p. 20.
[2] M.T. Robinson, J. Nucl. Mater. 216 (1994) 1.
[3] R.E. Stoller, MRS Symp. Proc. 373 (1995) 21.
[4] A.F. Calder, D.J. Bacon, J. Nucl. Mater. 207 (1993) 25.
[5] W.J. Phythian, R.E. Stoller, A.J.E. Foreman, A.F. Calder, D.J. Bacon, J. Nucl. Mater. 223 (1995) 245.
[6] T. Diaz de la Rubia, N. Soneda, M.J. Caturla, E.A. Alonso, J. Nucl. Mater. 251 (1997) 13.
[7] G.R. Odette, MRS Symp. Proc. 373 (1995) 137.
[8] G.R. Odette, B.D. Wirth, J. Nucl. Mater. 251 (1997) 157.
[9] B.D. Wirth, G.R. Odette, MRS Symp. Proc. 538, 1999, in press.

[10] M.L. Jenkins, M.A. Kirk, W.J. Phythian, J. Nucl. Mater. 205 (1993) 16.
[11] G.R. Odette, Neutron Irradiation Effects in Reactor Pressure Vessel Steels and Weldments, IAEA IWG-LMNPP-98/3, International Atomic Energy Agency, Vienna, 1998, p. 438.
[12] R.E. Stoller, in: A.S. Kumar, D.S. Gelles, R.K. Nanstad, E.A. Little (Eds.), Proceedings of the Conference on Effects of Radiation on Materials ASTM STP 1175, American Society for Testing and Materials, Philadelphia, 1993, p. 394.
[13] R.J. DiMelfi, D.E. Alexander, L.E. Rehn, J. Nucl. Mater. 252 (1998) 171.
[14] H. Trinkaus, B.N. Singh, A.J.E. Foreman, J. Nucl. Mater. 251 (1997) 172.
[15] P.T. Heald, Philos. Mag. 31 (1975) 551.
[16] W.G. Wolfer, Fundamental Aspects of Radiation Damage in Metals, CONF-751006-P2, US National Technical Information Service, Springfield, VA, 1975, p. 812.
[17] B.D. Wirth, G.R. Odette, D. Maroudas, G.E. Lucas, J. Nucl. Mater. 244 (1997) 185.
[18] B.D. Wirth, G.R. Odette, D. Maroudas, G.E. Lucas, MRS Symp. Proc. 504 (1998) 63.
[19] B.D. Wirth, PhD dissertation, University of California, Santa Barbara, 1998.
[20] R.E. Stoller, G.R. Odette, B.D. Wirth, J. Nucl. Mater. 251 (1997) 49.
[21] B.D. Wirth, G.R. Odette, D. Maroudas, G.E. Lucas, Structure and energetics of self-interstitial clusters in α-iron, Philos. Mag. A, to be submitted.
[22] Y.N. Osetsky, M. Victoria, A. Serra, S.I. Golubov, V. Priego, J. Nucl. Mater. 251 (1997) 34.
[23] Y.N. Osetsky, personal communication.
[24] A.V. Barashev, Y.N. Osetsky, D.J. Bacon, On the mechanism of interstitial cluster migration in alpha-iron, presented at 1998 MRS Fall Meeting, Microstructural Processes in Irradiated Materials Symposium.
[25] M.W. Finnis, J.E. Sinclair, Philos. Mag. A 50 (1984) 45.
[26] D. Maroudas, R.A. Brown, Phys. Rev. B 47 (1993) 15562.
[27] M.W. Finnis, MOLDY 6, UKAEA Harwell Laboratory, AERE R-13182, 1988.
[28] J.P. Hirth, J. Lothe, Theory of Dislocations, 2nd ed., Krieger, Malabar, FL, 1992.
[29] J.O. Schiffgens, K.E. Garrison, J. Appl. Phys. 43 (8) (1972) 3240.
[30] R.L. Fleischer, D. Peckner (Eds.), Strengthening of Metals and Alloys, Reinhold, New York, 1964, p. 93.